

# Sparsity-based Iris Classification using Iris Fiber Structures

N. Pattabhi Ramaiah, C. Krishna Mohan  
Department of Computer Science and Engineering  
Indian Institute of Technology Hyderabad, India, Pin: 502205  
Email: ramaiah.iith@gmail.com, ckm@iith.ac.in

N. Srilatha  
BnPRs Research Lab  
Andhrapradesh, India, Pin: 533222  
Email: srilatha@bnprs.in

**Abstract**—As there is a growing demand for biometrics usage in e-Society, the biometric recognition system faces the scalability issue as the number of people to be enrolled into the system runs into billions. In this paper, we propose an approach for iris classification using three different iris classes based on iris fiber structures, namely, stream, flower, jewel and shaker for faster retrieval of identities in large scale biometric system. A sparsity based on-line dictionary learning (ODL) algorithm is used in the proposed classification approach where dictionaries are developed for each class using log-Gabor wavelet features. Also, a method for iris adjudication process is illustrated using the iris classification to reduce the search space. The efficacy of the proposed classification approach is demonstrated on the standard UPOL iris database.

## I. INTRODUCTION

Among all the biometrics, fingerprints and iris give more accurate results in uniquely identifying the people based on minutia features. However, the biometric system allows few errors in identification with a threshold at equal error rate. In order to reduce the errors, fingerprint experts look for possible fingerprint matches and enhance the fingerprints to compare the minutia features manually using fingerprint adjudication process. Fingerprint adjudication means, comparison of two fingerprints side-by-side to analyze the matched minutia features. Even though the iris biometric is more accurate than the fingerprints, there is a need for iris adjudication process in civilian applications. Also, there are scalability issues with the large scale biometric systems where a classification approach is required to reduce the search space.

The complex iris texture provides the uniqueness for iris images. Daugman proposed an iris recognition system by using gabor filters and iris codes [6], [3], [4], [5]. Several other researches including Wildes [24], Boles and Boashash [2] proposed different iris recognition algorithms by representing the iris texture with Laplacian pyramid construction and 1D wavelet transform, respectively. Few researchers already explored iris classification techniques using hierarchical visual codebook [23], block-wise texture analysis [21] and color information [25], [18]. So far, there is no classification approach based on the pre-defined iris classes.

Sparse representation has received a lot of attention from researchers in signal and image processing. Sparse coding involves the representation of an image as a linear combination of some atoms in a dictionary [19]. Several algorithms like on-line dictionary learning (ODL) [15],  $K$ -SVD [1] and method of optimal directions (MOD) [10] have been developed to

process training data. Sparse representation is used to match the input query image with the appropriate class. Etemand and Chellappa [11] proposed a feature extraction method for classification using wavelet packets. In [22], a method presented for the learning of dictionaries simultaneously. Recently, similar algorithms for simultaneous sparse signal representation have also been proposed [20], [13]. The on-line dictionary learning algorithm alternates between sparse coding and dictionary update steps. Several efficient pursuit algorithms have been proposed in the literature for sparse coding [10],[16]. The simplest one is the  $l_1$ -lasso algorithm [14]. Main advantage with ODL algorithm is its computational speed as it uses  $l_1$ -lasso algorithm for sparse representation.

The rest of the paper is organized as follows: In section II, the proposed iris classification approach and the details of on-line dictionary learning are presented. Experimental results of the proposed classification and adjudication framework are given in section III. Conclusions are explained in section IV.

## II. PROPOSED IRIS CLASSIFICATION AND ADJUDICATION FRAMEWORK

The proposed iris classification approach uses three different classes of iris images [12] namely, stream, flower, and jewel-shaker as illustrated in Figure 1. The iris structure can be determined by the arrangement of white fibers radiating from the pupil. In stream iris structure, these fibers are arranged in regular and uniform fashion. The arrangement of fibers is irregular in the flower iris structure. In jewel iris structure, the fibers have some dots. The shaker iris structure have both the characteristics of flower and jewel iris structures. The jewel and shaker classes are merged due to rare occurrence and to make the classification proportional among all the pre-defined classes. The arrangement of fibers are illustrated in Figure 2.

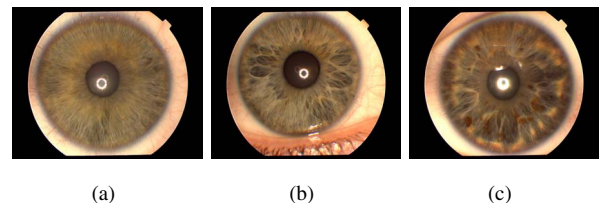


Fig. 1. Iris classes: (a) stream, (b) flower and (c) jewel-shaker structures.

The following are the steps involved in the proposed iris classification and adjudication framework:

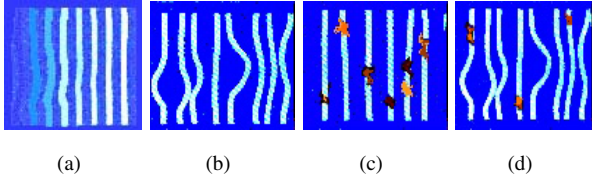


Fig. 2. Iris fibers: (a) stream, (b) flower, (c) jewel and (d) shaker fibers.

**Step 1. Iris segmentation and normalization** : The pupillary and limbic boundaries [17] of an iris image are approximated as circles using three parameters: the radius  $r$ , and the coordinates of the center of the circle,  $x_0$  and  $y_0$ . The integrodifferential operator [6] used for iris segmentation is:

$$\max_{r, x_0, y_0} G_\sigma(r) * \frac{\partial}{\partial r} \int_{r, x_0, y_0} \frac{I(x, y)}{2\pi r} ds, \quad (1)$$

where  $G_\sigma(r)$  is a smoothing function and  $I(x, y)$  is the image of the eye.

After applying the operator, the resultant segmented iris image is as shown in Figure 3. The segmented iris image is then converted to a dimensionless polar coordinate system based on the Daugman Rubber Sheet model [6] as shown in Figure 4.

**Step 2. Feature extraction** [17]: The log-Gabor wavelet feature vector of size  $240 \times 20$  is extracted from the normalized iris image of size  $120 \times 20$ . The resultant feature vector is converted to a single column vector by column major ordering. From each class, some of the iris images are selected to express as a linear weighted sum of the feature vectors in a dictionary belonging to three different classes of iris.

**Step 3. Iris classification using ODL**: An on-line dictionary learning (ODL) algorithm is used to classify the iris data into three different classes to reduce the search space. The weights associated with feature vectors in the dictionary are evaluated using ODL algorithm, which is a solution to  $l_1$  optimization for over-determined system of equations. The feature vectors which belong to a particular iris class carry significant weights which are non-zero maximum values.

The class  $C = [C_1, \dots, C_N]$  consists of training samples collected directly from the image of interest. In the proposed sparsity model, images belonging to the same class are assumed to lie approximately in a low dimensional subspace. Given  $N$  training classes, the  $p^{th}$  class has  $K_p$  training images  $\{\mathbf{y}_i^N\}_{i=1, \dots, K_p}$ . Let  $b$  be an image belonging to the  $p^{th}$  class, and it is represented as a linear combination of these training samples:

$$b = \mathbf{D}^p \Phi^p, \quad (2)$$

where  $\mathbf{D}^p$  is a dictionary of size  $m \times K_p$ , whose columns are the training samples in the  $p^{th}$  class and  $\Phi^p$  is a sparse vector. The following are the steps involved in the proposed classification method:

- 1) **Dictionary Construction**: Construct the dictionary for each class of training images using on-line dictionary learning algorithm [15]. Then, the dictionaries  $D = [D_1, \dots, D_N]$  are computed using the equation:

$$(\hat{\mathbf{D}}_i, \hat{\Phi}_i) = \arg \min_{\mathbf{D}_i, \Phi_i} \frac{1}{N} \sum_{i=1}^N \frac{1}{2} \|\mathbf{C}_i - \mathbf{D}_i \Phi_i\|_2^2 + \lambda \|\Phi_i\|_1, \quad (3)$$

satisfying  $\mathbf{C}_i = \hat{\mathbf{D}}_i \hat{\Phi}_i$ ,  $i = 1, 2, \dots, N$ .

- 2) **Classification**: In this classification process, the sparse vector  $\Phi$  for given test image is found in the test dataset  $B = [b_1, \dots, b_t]$ . Using the dictionaries of training samples  $D = [D_1, \dots, D_N]$ , the sparse representation  $\Phi$  satisfying  $D\Phi = B$  is obtained by solving the following optimization problem:

$$\Phi^j = \arg \min_{\Phi} \frac{1}{2} \|\mathbf{b}_j - \mathbf{D} \Phi_j\|_2^2; \quad (4)$$

subject to  $\|\Phi_j\|_1 \leq T_1$ , and  $\hat{i} = \arg \min_i \|\mathbf{b}_j - \mathbf{D} \delta_i(\Phi^j)\|_2^2$ ,  $j = 1, \dots, t$ .

where  $\delta_i$  is a characteristic function that selects the coefficients. Then  $b_j$  is assigned to  $C_i$  associated with the  $i^{th}$  dictionary. It means, finding the sparsest dictionary for a given test data using  $l_1$ -lasso algorithm. Then, test data is assigned to the class associated with this sparsest dictionary.

**Step 4. Iris Adjudication**: The matched iris pairs are compared using the adjudication process to illustrate the match-ability of iris images based on the similarity of iris regions marked with three different colors, namely, green, yellow and red. The green, yellow and red colors indicate good, poor and bad match, respectively. The normalized iris image is divided into different regions and the confidence-level of matching for each region is verified and assigned a color code using the dissimilarity measurement.

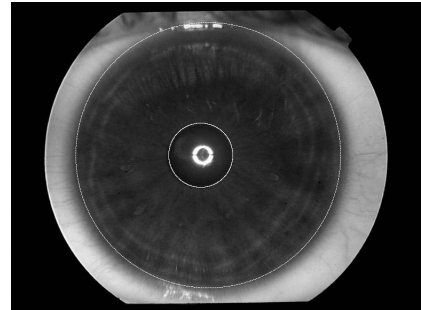


Fig. 3. Iris image segmentation



Fig. 4. Normalized Iris Image

### III. EXPERIMENTAL RESULTS

The experiments were conducted using the iris images taken from the standard UPOL iris database [9], [8], [7]. The iris data is collected from 64 subjects, with three samples of left and right eyes from each subject resulting in a total

of 384 iris images. Each iris image is of 24 bit RGB color space with a high resolution image size,  $768 \times 576$ . The images were captured using the optical device (TOPCON TRC501A) which is connected to a Sony DXC-950p 3CCD camera. In the proposed iris classification approach, three classes are manually identified using the iris patterns stream, flower and jewel-shaker as shown in Table I. These classes are categorized based on the iris fiber structures (texture information), so the images were converted to gray-scale images for further processing. The manual identification of the predefined classes is not required for all the data in large-scale applications, but at least those classes should be identified for the training samples.

TABLE I. IRIS CLASSES DEFINED BASED ON THE IRIS FIBERS STREAM, FLOWER AND JEWEL-SHAKER

Class	# of Images (%)	Subject Ids
Class-1 (Stream)	192 (50%)	001,006,007,008,011,013,014,016,018,019,020,021,023,024,026,027,028,033,041,042,044,045,050,051,052,053,058,059,060,061,062,064
Class-2 (Flower)	102 (26.56%)	002,009,010,015,017,022,031,036,037,040,043,047,048,049,054,056,063
Class-3 (Jewel-Shaker)	90 (23.44%)	003,004,005,012,025,029,030,032,034,035,038,039,046,055,057

In order to evaluate the accuracy of proposed classification approach using on-line dictionary learning, the database is split into three sets: training set, testing set and validation set. The distribution of all the three sets are taken in such a way that the 2 samples of each iris image is allotted to the training set and validation set, and the remaining iris sample is given to the test set. The training set consists of 224 images where 112 images are from Class-1 (Stream), 60 images are from Class-2 (Flower) and 52 images are from Class-3 (Jewel-Shaker). The number of test images selected from Class-1, Class-2 and Class-3 are 64, 34 and 30, respectively. A set of 32 iris images is assigned to validation set where 16 images belong to Class-1, 8 images belong to Class-2 and 8 images belong to Class-3.

The experiments were conducted in three different ways of choosing test sets (systematically selecting first, second or third samples of each iris) where the accuracy is almost similar. The classification accuracy is shown for the test data set with different dictionary sizes 60, 90 and 120, in Tables II, III and IV, respectively.

TABLE II. CLASSIFICATION ACCURACY ON TEST DATA SET FOR DICTIONARY SIZE = 60

Class	Residual Parameter		
	0.5	<b>0.05</b>	0.005
Class-1 (Stream)	90.5	<b>97</b>	93.83
Class-2 (Flower)	91.18	<b>94.12</b>	88.2
Class-3 (Jewel-Shaker)	100	<b>100</b>	100

TABLE III. CLASSIFICATION ACCURACY ON TEST DATA SET FOR DICTIONARY SIZE = 90

Class	Residual Parameter		
	0.5	<b>0.05</b>	0.005
Class-1 (Stream)	95	<b>100</b>	98.5
Class-2 (Flower)	94.12	<b>100</b>	97.06
Class-3 (Jewel-Shaker)	100	<b>100</b>	100

TABLE IV. CLASSIFICATION ACCURACY ON TEST DATA SET FOR DICTIONARY SIZE = 120

Class	Residual Parameter		
	0.5	<b>0.05</b>	0.005
Class-1 (Stream)	95	<b>100</b>	98.5
Class-2 (Flower)	91.18	<b>100</b>	96.06
Class-3 (Jewel-Shaker)	100	<b>100</b>	100

In Table V, the classification accuracy for the validation data set is given. It is observed that 100% classification accuracy is achieved for the dictionary sizes 90 and 120 with residual error value 0.05 as shown in Figure 5. The confusion matrices for both test data and validation data sets are shown in Table VI.

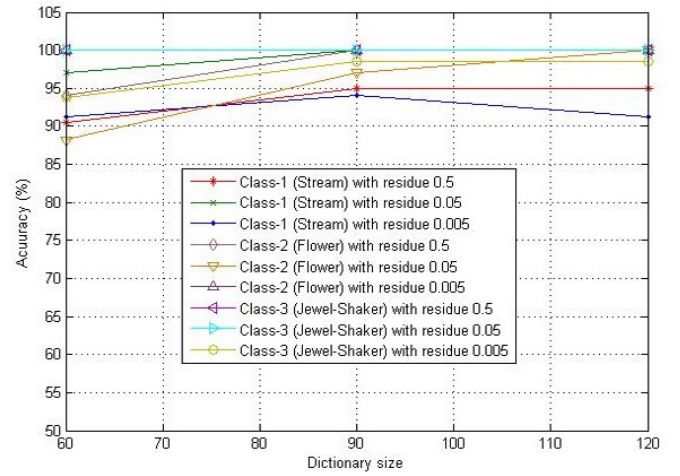


Fig. 5. Classification accuracy for different dictionary sizes 60, 90 and 120

TABLE V. CLASSIFICATION ACCURACY ON VALIDATION DATA SET

Class	Dictionary Sizes		
	60	<b>90</b>	120
Class-1 (Stream)	91.66	<b>100</b>	100
Class-2 (Flower)	100	<b>100</b>	100
Class-3 (Jewel-Shaker)	100	<b>100</b>	100

TABLE VI. CONFUSION MATRIX FOR TEST AND VALIDATION DATA

Class	Testing set			Validation set		
	C1	C2	C3	C1	C2	C3
C1	64	0	0	16	0	0
C2	0	34	0	0	8	0
C3	0	0	30	0	0	8

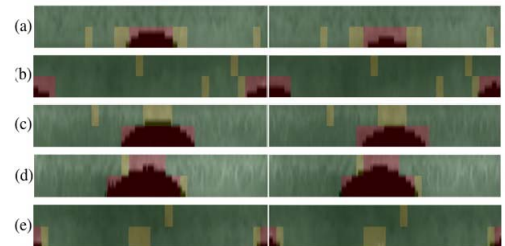


Fig. 6. Iris adjudication: genuine iris matches with hamming distances (a) 0.21, (b) 0.19, (c) 0.16, (d) 0.15, (e) 0.19

The adjudication results for genuine iris matches are illustrated in Figure 6 and for the impostor iris matches are

given in Figure 7. The normalized images shown on these figs are taken from CASIA database for better illustration of adjudication process.

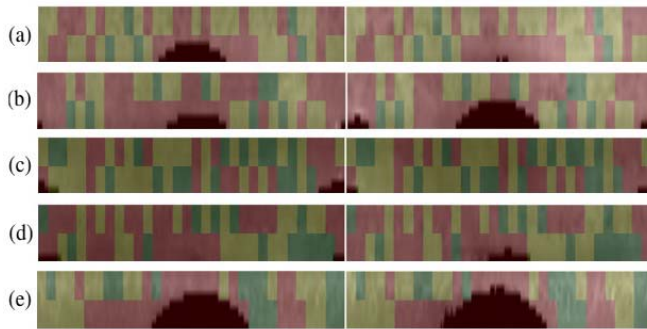


Fig. 7. Iris adjudication: impostor iris matches with hamming distances (a) 0.48, (b) 0.46, (c) 0.43, (d) 0.51, (e) 0.37

#### IV. CONCLUSIONS AND FUTURE WORK

In this paper, a new methodology for iris classification is proposed to classify the iris images into three different classes namely stream, flower and jewel-shaker. The ability of on-line dictionary learning (ODL) to achieve sparse representation of an image is exploited to develop dictionaries for each class using log-gabor wavelet features. The proposed classification approach achieved 100% classification accuracy with dictionary size 90 and residual error 0.05. Finally the adjudication results are illustrated to avoid the identification errors. The proposed method addressed the scalability issue in large scale iris biometric recognition system for faster retrieval of identities. The proposed approach can be applied in large scale biometric system in order to reduce the search space and faster retrieval of identities. The manual identification of the predefined classes is not required for all the data in large-scale applications, but at least those classes should be identified for the training samples. The data used for iris classification was collected under visible illumination. Most of the iris recognition systems use the data acquired at near infra-red (NIR) wavelengths. These systems are more accurate among all the existing biometric recognition systems. It is very hard to label the iris classes in the available standard near infra-red databases. The same experimental setup should be executed for the near infra-red iris database which have more texture information to distinguish the iris labels.

#### REFERENCES

- [1] M. Aharon, M. Elad, and A. Bruckstein. The k-svd: An algorithm for designing overcomplete dictionaries for sparse representation. *Signal Processing, IEEE Transactions on*, 54(11):4311–4322, 2006.
- [2] W. W. Boles and B. Boashash. A human identification technique using images of the iris and wavelet transform. *Signal Processing, IEEE Transactions on*, 46(4):1185–1188, 1998.
- [3] J. Daugman. Statistical richness of visual phase information: update on recognizing persons by iris patterns. *International Journal of computer vision*, 45(1):25–38, 2001.
- [4] J. Daugman. Demodulation by complex-valued wavelets for stochastic pattern recognition. *International Journal of Wavelets, Multiresolution and Information Processing*, 1(01):1–17, 2003.
- [5] J. Daugman. How iris recognition works. *Circuits and Systems for Video Technology, IEEE Transactions on*, 14(1):21–30, 2004.
- [6] J. G. Daugman. High confidence visual recognition of persons by a test of statistical independence. *Pattern Analysis and Machine Intelligence, IEEE Transactions on*, 15(11):1148–1161, 1993.

- [7] M. Dobe and L. Machala. Upol iris database. <http://www.inf.upol.cz/iris/>, 2004.
- [8] M. Dobeš, L. Machala, P. Tichavský, and J. Pospíšil. Human eye iris recognition using the mutual information. *Optik-International Journal for Light and Electron Optics, 2004 Elsevier journal on*, 115(9):399–404, 2004.
- [9] M. Dobeš, J. Martinek, D. Skoupil, Z. Dobešová, and J. Pospíšil. Human eye localization using the modified hough transform. *Optik-International Journal for Light and Electron Optics, 2006 Elsevier journal on*, 117(10):468–473, 2006.
- [10] K. Engan, S. O. Aase, and J. Hakon Husoy. Method of optimal directions for frame design. *Acoustics, Speech, and Signal Processing, 1999. Proceedings., 1999 IEEE International Conference on*, 5:2443–2446, 1999.
- [11] K. Etemad and R. Chellappa. Separability-based multiscale basis selection and feature extraction for signal and image classification. *Image Processing, IEEE Transactions on*, 7(10):1453–1465, 1998.
- [12] U. Foundation. The rayid model of iris interpretation. <http://rayid.com/main/structures.asp>, 2009.
- [13] K. Huang and S. Aviyente. Sparse representation for signal classification. *NIPS*, pages 609–616, 2006.
- [14] H. Lee, A. Battle, R. Raina, and A. Y. Ng. Efficient sparse coding algorithms. *Advances in neural information processing systems, 2007 MIT Transactions on*, 19:801, 2007.
- [15] J. Mairal, F. Bach, J. Ponce, and G. Sapiro. Online dictionary learning for sparse coding. *Machine Learning, 2009 ACM Conference on*, pages 689–696, 2009.
- [16] S. G. Mallat and Z. Zhang. Matching pursuits with time-frequency dictionaries. *Signal Processing, IEEE Transactions on*, 41(12):3397–3415, 1993.
- [17] L. Masek et al. Recognition of human iris patterns for biometric identification. *Bachelor's thesis, University of Western Australia*, 2003.
- [18] I. Pavaloj, A. Ciobanu, and M. Luca. Iris classification using winicd and lab color features. In *E-Health and Bioengineering Conference (EHB), 2013*, pages 1–4. IEEE, 2013.
- [19] I. Ramirez, P. Sprechmann, and G. Sapiro. Classification and clustering via dictionary learning with structured incoherence and shared features. *Computer Vision and Pattern Recognition (CVPR), 2010 IEEE Conference on*, pages 3501–3508, 2010.
- [20] F. Rodriguez and G. Sapiro. Sparse representations for image classification: Learning discriminative and reconstructive non-parametric dictionaries. 2008.
- [21] A. Ross and M. S. Sunder. Block based texture analysis for iris classification and matching. *Computer Vision and Pattern Recognition Workshops (CVPRW), 2010 IEEE Computer Society Conference on*, pages 30–37, 2010.
- [22] P. Sprechmann and G. Sapiro. Dictionary learning and sparse coding for unsupervised clustering. *Acoustics Speech and Signal Processing (ICASSP), 2010 IEEE International Conference on*, pages 2042–2045, 2010.
- [23] Z. Sun, H. Zhang, T. Tan, and J. Wang. Iris image classification based on hierarchical visual codebook. *Pattern Analysis and Machine Intelligence, IEEE Transactions on*, 2013.
- [24] R. P. Wildes. Iris recognition: an emerging biometric technology. *Proceedings of the IEEE*, 85(9):1348–1363, 1997.
- [25] H. Zhang, Z. Sun, T. Tan, and J. Wang. Iris image classification based on color information. *Pattern Recognition (ICPR), 2012 21st International Conference on*, pages 3427–3430, 2012.